Systematic Design of a Cross-Polarized Dermoscope for Visual Inspection and Digital Imaging

Hening Wang, Xin Xu, Xiaoqin Li, Peng Xi, and Qiushi Ren

A dermoscope is a diagnostic device that can image the skin *in situ* and is used for early diagnosis of melanoma and pigmented skin lesions. In this paper, we describe the design and construction of a cross-polarized dermoscope including the illumination evaluation, imaging design, and the mechanical setup. By using the cross-polarization dermoscope, specular reflection from the superficial layer of the skin is largely eliminated. Therefore, deeper layers of the skin, such as the inner pigments and the capillary blood vessels, can be visualized.

Introduction

Skin, as the largest organ of our body, plays an important role in protecting deeper tissues from damage by the external environment. The incidence of skin cancer is increasing each year; therefore, tools to examine skin lesions are of great importance. Early detection of skin cancers leads to effective treatment and thus a high cure rate [1]. However, common clinical diagnostic methods, such as biopsy-pathological analyses, are restricted in the case of dermal examinations due to their invasive nature.

One of the important functions of the superficial layer of the skin is to reflect light for shielding of the underlying structures [2]. This causes difficulties for physicians in their attempts to visualize the deeper tissues for diagnosis. Nevertheless, optical methods can provide in-depth diagnostic imaging modalities, and diagnoses utilizing polarized light and *in vivo* imaging of skin cancer have been reported [3]-[5] . The use of polarized light to characterize cells and tissues has a long history in medicine and biology, beginning with studies of cell suspensions and, more recently, studies of turbid tissue phantoms and tissues *in vivo* [6]. In addition, polarized light imaging has been used to detect the borders of skin cancers that are not visible to the naked eye, thus facilitating assessment of cancer boundaries [6], [7]. A number of camera systems utilizing polarized light have been used in clinical practice for assessing skin cancer margins and to reduce surgery time and patient discomfort [8]-[10].

Because of the light scattering nature of biological tissues, the polarization angle is altered for scattering caused by the deeper layers, while the superficial back scattered light maintains its polarization status. Badizadegan, et al. used this phenomenon to image human epithelial tissue properties with polarized light-scattering spectroscopy, and this method can be used to detect precancerous lesions in optically accessible organs [11]. Yaroslavsky et al. developed a novel, multispectral, dye-enhanced polarized light imaging technique that enabled rapid imaging of large tumor fields and thus has significant potential as a guidance tool in tumor excision surgery [12]. Burns et al. improved the contrast of sub-retinal structures by using polarization analysis and thereby increased the clinician's ability to detect

When used to evaluate melanomas and other pigmented skin lesions, the dermoscope magnifies a pigmented lesion and allows the dermatologist to see through the stratum corneum, thereby permitting a detailed view of the deep structural information of the skin...

This research is supported by the National Basic Research Program of China ("973" Program, 2010CB933901, 2011CB707500, 2011CB809101), the National Natural Science Foundation of China (60808029, 61178076), Shanghai Jiao Tong University Med-Engineering Fund (YG2009ZD201), and Peking University Med-Engineering Fund.

1094-6969/11/$25.00©2011IEEE

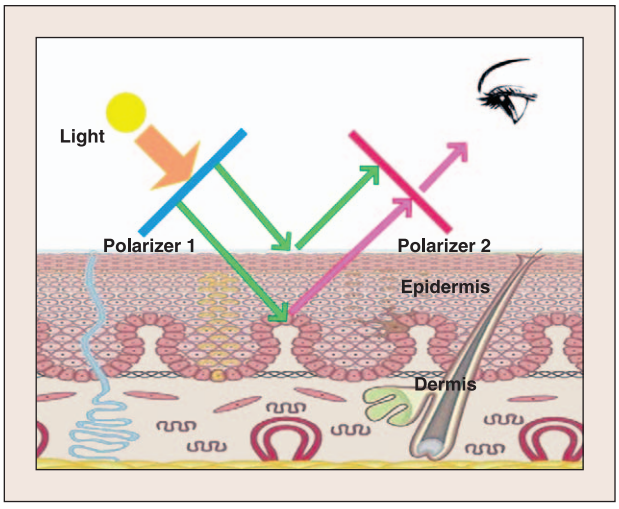

Fig. 1. Schematic diagram of the principles of a cross-polarization dermoscope.

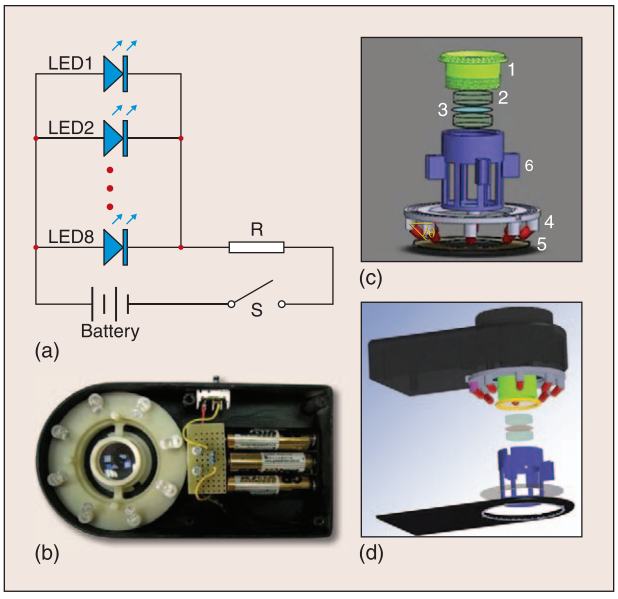

Fig. 2. Circuit and mechanical design of the dermoscope: (a) circuit design, (b) the dermoscope system prototype, (c) an illustration of the mechanical design and main components of the optical system, and (d) the CAD assembly of the dermoscope.

and quantify early retinal changes associated with aging [13].

In this paper, we describe the cross-polarization dermoscope, an instrument that can be used to obtain dermal images from the deep layers of the skin. The dermoscope is a non-invasive instrument that images skin lesions beneath the superficial skin layer. When used to evaluate melanomas and other pigmented skin lesions, the dermoscope magnifies a pigmented lesion and allows the dermatologist to see through the stratum corneum, thereby permitting a detailed view of the deep structural information of the skin [14]. An oil-immersion dermoscope traditionally consists of a magnifier (typically 10x), a non-polarized light source, a transparent plate, and a liquid medium between the instrument and the skin. The reflection from the skin surface is reduced by daubing sufficient oil on the skin to match the refractive index of the plate [15]. However, in practice, the messy nature of the oil is inconvenient. To eliminate the use of oil, cross-polarization was applied in conjunction with the dermoscope in this work.

The aim of the cross-polarization dermoscope is to aid the physician to diagnose the melanoma with a deeper penetration depth imaging. It has to be compared with a common dermoscope, and sets of post evaluations (such as biopsies) have to be applied to a relatively large number of patients and diagnosed by one doctor (or doctors with the same experience) to avoid bias, to obtain the sensitivity and specificity of this cross-polarization tool. Because the focus of this article is on the instrumentation of the dermoscope, we didn't include these experiments.

System Design Simulation

The principle of a cross-polarization dermoscope is shown in Fig. 1. Cross-polarization detection is realized through the application of a pair of polarizers placed perpendicularly between the light source and the observer. The incident light passes through Polarizer 1 and illuminates the skin. Because the specular reflection from the surface maintains the same polarization as the incident light, it will be blocked by Polarizer 2 whose polarization direction is perpendicular to the incident light; however, the scattering of the light from the deep tissue structures alters its polarization, so that it can partially pass through the second polarizer for imaging [4], [5]. The design simulation of the cross-polarized dermoscope consists of three parts: electronic design and illumination evaluation, optical imaging design, and system mechanical design, and they are described in the following paragraphs. The CAD mechanical design and the optical simulation of the cross-polarization

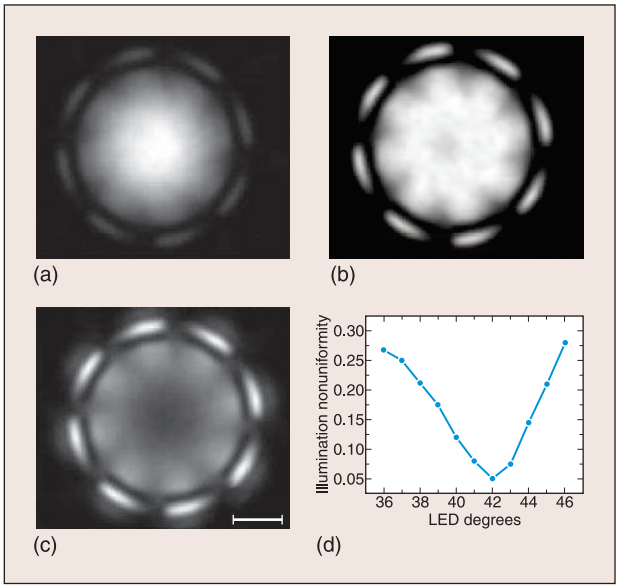

Fig. 3. Illumination distribution on the targeted surface with different LED θ angles from 16 mm: (a) θ =39°, (b) θ = 42°, (c) θ = 45° (scale bar = 10 mm), and (d) illumination nonuniformity versus LED angle in degrees.

dermoscope can be downloaded from_http://bme.pku.edu.cn/~xipeng/Tools.htm.

Illumination Evaluation

Eight white LED lights powered by batteries provide a uniform illumination of the targeted skin area selected for imaging and diagnosis. Three 1.5 V batteries are used with a resistance of 75 Ω to provide power for the LEDs. The light intensity at the skin surface was measured to be 32000 lux using a voltage of 3.3 V and thus, provided sufficient intensity to adequately illuminate the area (Fig. 2a).

Simulation of the illumination system was conducted to evaluate its uniformity. Analysis and optimization of the light performance required determination of the LED parameters necessary for uniform illumination. OptisWorks (OPTIS, La Farléde, France) was used to simulate illumination and light transmission. Ray tracing was performed in the 3D view of the SolidWorks environment (DS Solidworks, MA, USA) to simulate the propagation of rays emitted by the source and provided a light simulation based on a physical model.

The surface source in the LED model was defined first to simulate the light source for ray tracing. The power of the source was defined as 323.58 Lumen and equal to the value measured by a photometer. The emittance, which describes how each point of a surface emits rays, was set to a uniform pattern. A Lambertian intensity model was selected to simulate the directions of light emission and limit the lighting diagram to a cone and was achieved by applying the half angle value given in the LED product specifications. The LEDs in the packing ring formed a half angle equal to 15° (θ; shown in Fig. 2c), and this value minimized the scattered light leaking out of the polarizer. The optical properties in each assembly include surface quality and internal and external material. Ray tracing filters aided in the selection of certain facets of the system by displaying rays that were transmitted or blocked.

A 2D detector was then added to the system to compute the irradiance (Lux) arriving at the targeted surface and the distribution of luminous intensity. The results indicated that uniformity and efficiency of the illumination were influenced by the angle of the LEDs and the distance between the LEDs and the skin surface. Small angles and closer placement of the LEDs to the skin gave brighter illumination of the central area (Fig. 3a), while larger angles and a more distant placement gave a smoother illumination. An excessive angle increased the light emission that was directed towards the sidewall of the dermoscope resulting in a lower illumination of the targeted surface (Fig. 3c).

Finally, the integral of the nonuniformity U_I of the illumination in the field of view (FOV), diameter = 10 mm, was analyzed using MATLAB and calculated as:

$$U_I = \frac{I_{\max} - I_{\min}}{I_{\max} + I_{\min}} \quad (1)$$

where I_{max} and I_{min} respectively denote the maximum and minimum intensity inside the FOV. Smaller U_I values produce better illumination uniformity. The uniformly bright area, U_I < 10%, seen in Fig. 3b is twice that of the bright area in Fig. 3a

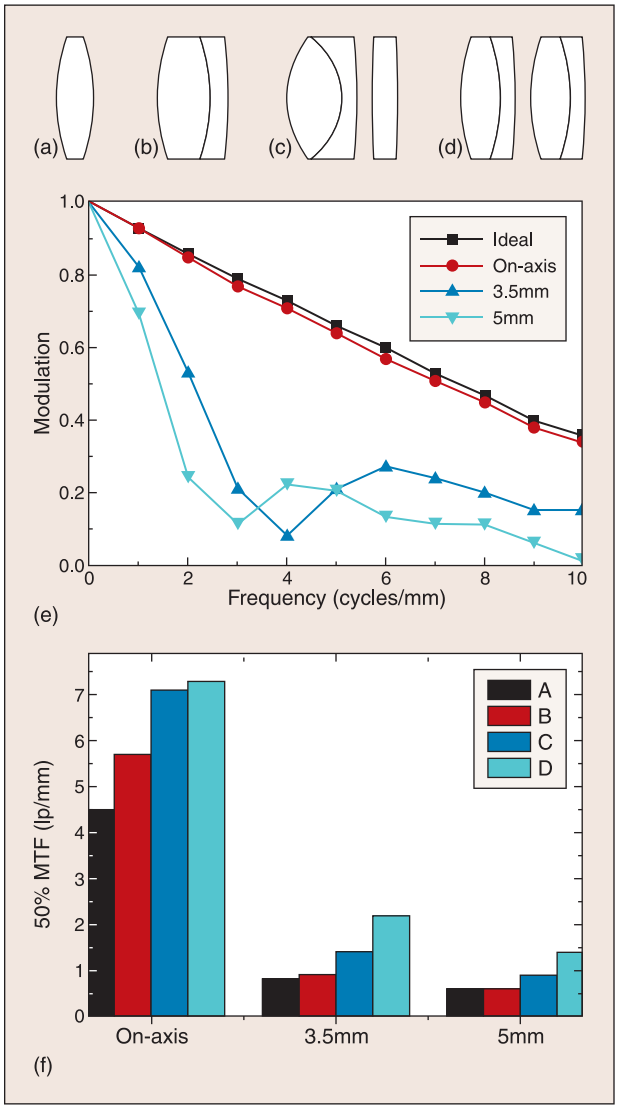

Fig. 4. Optimization of lens type used in the dermoscope. (a) Group A – single lens, (b) Group B – double lens, (c) Group C – single plus double lens, (d) Group D – two double lenses, (e) a typical MTF curve versus image quality using (d), and (f) the 50% MTF value comparison at on-axis with a radius of 3.5 mm or 5 mm.

leading to an increase in image sharpness and allows the dermoscope to have a wide-field imaging capacity.

Figure 3d illustrates the relationship of U_I and the LED angle θ. When θ is 42°and the distance between the LED surface and the targeted surface is 16 mm, a uniform illumination was achieved with the LEDs. These parameters were used to set the imaging and mechanical system design conditions.

Imaging Design

A simple magnifying lens, e.g., 10x, may lead to serious image aberrations, and the edges are easily blurred when compared with the central FOV. The choice of an optimal eyepiece for the dermoscope was made by evaluating the image quality obtained from various combinations of lenses using Optics Software for Layout and Optimization software (OSLO EDU) from Lambda Research, MA, USA, which provided an optical

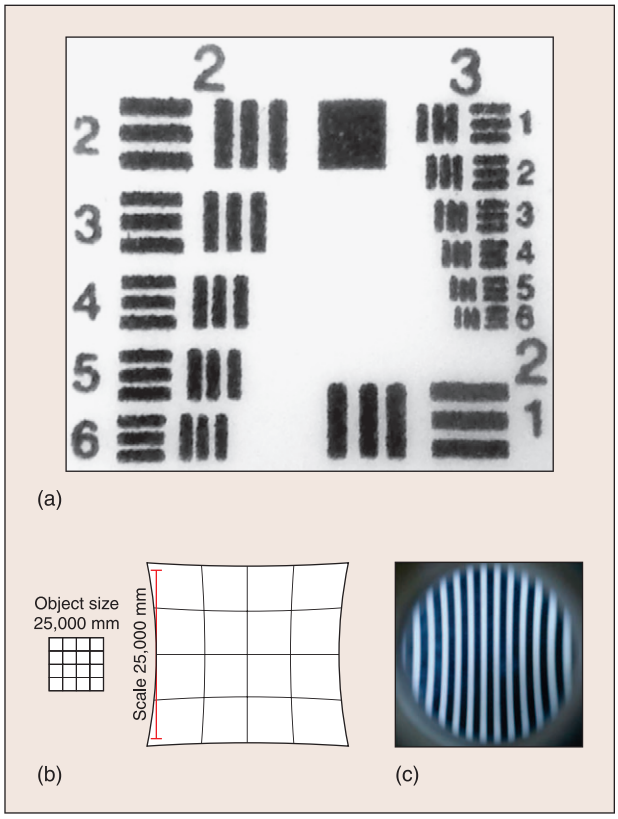

Fig. 5. Image resolution and distortion. (a) The USAF resolution target imaged with the dermoscope. (The width of the target is 15mm.) (b) The evaluation of the image distortion of the dermoscope with OSLO optical simulation, and (c) an image of a bar object with 0.5 lp/mm.

design environment for the simulation and evaluation of different combinations of lenses.

Because the comfortable viewing distance for the human eye is 250 mm, the object distance from the dermoscope to the skin surface u can be calculated from:

$$\frac{1}{f}=\frac{1}{u}+\frac{1}{v} \tag{2}$$

where f refers to the focal distance of the dermoscope and v is the image distance (-250 mm). Thus, the magnification (MAG) $=-\frac{v}{u}=10$, u = 25 mm and f = 27.8 mm. Several focal distance configurations were tested with commercially available lenses (see Fig. 4): (a) Group A – single lens (f = 30 mm); (b) Group B – double lens (f = 30 mm); (c) Group C – the group of lenses consisting of one doublet (f = 30 mm) and one single lens (f = 200 mm); and (d) Group D – the group of lenses combining two double lenses (f = 50 mm).

Performance evaluation and comparisons were obtained using half the value of the modulation for on-axis (center of the FOV) and off-axis (edge of the FOV) performance and the modulation transfer function (MTF) diagrams of the four lens combinations (Fig. 4e). The MTF was plotted as a function of image frequency and showed that a larger MTF value at any given frequency represented an image with better contrast.

Group D lenses had the largest MTF values, both on-axis and off-axis, and therefore were chosen as the prototype model for the design. Note that the 50% MTF (Fig. 4f) was only used for performance comparison between the lens groups.

The common measurement standard of 10% or 5% MTF is related to the finest structure that can be resolved, which may cause ambiguity when a lens (group) has a longer tail on the MTF curve. We, therefore, chose 50% MTF value as a relative evaluation of the lens groups to concentrate on the performance of the lens with its power to resolve details with relatively high contrast (modulation). Although these evaluations should be the same if the MTF curves contain the same shape, the 50% MTF comparison can preserve more contrast, which may be useful for diagnosis.

The US Air Force 1951 Resolution Target (EdmundOptics NT38-710) was also used to test the resolving power of the optical imaging system incorporated in our dermoscope design (Fig. 5a). The resolution target was categorized into three groups with six elements per group. The scales and dimensions of the bars are given by the expression:

$$\text{Resolution (lp/mm)} = 2^{\text{Group} + (\text{element} - 1)/6} \tag{3}$$

where lp/mm refers to line pairs per mm. It is clear from Fig. 5 that the system can easily resolve the smallest target resolution (Group 3 Element 6). This implies that the resolution of the dermoscope is greater than 14.3 lp/mm. The image obtained by the camera only (without the dermoscope) was only able to resolve structure at the Group 2 Element 2 target level, and this corresponded to 4.49 lp/mm.

Additional simulations of lens aberration using a pixelated grid or bar source (Fig. 5b) show the field curvature and distortion at the edge of the FOV. The resolution can be increased by also applying a diaphragm so that only the central part of the lens is utilized. The position of the diaphragm should be placed in the conjugation plane with the skin, so that the border of the diaphragm does not cause blur in the border during imaging. To minimize the complexity of our dermoscope, it is not included in our design.

Mechanical Design

The mechanical design is shown in Fig. 2b-d. A cuboid body is joined to the cylindrical head for easy handling. The electrical system is fixed inside the body, with the circuit board in the middle and the on-off switch on the side. A battery clip and cover are also located on the back for easy battery replacement.

The main optical component of the dermoscope consists of two double lenses that are used as the magnifying components (described in the previous section; Figs. 2c and d). Two polarizing filters are employed, one of which (part 5) is placed in front of the LEDs (part 4) while the other (part 3) is placed between the pair of double lenses. In practice, the second cross-polarization analyzer can be placed anywhere, just as long as the reflected light passes through it before arriving at the observer. The lenses (part 2) are placed in an adjustable focus knob (part 1) and extractable circular mount, which is used for mounting the imaging camera (not shown in the figure). By twisting the circular mount, which is connected with shot through threads

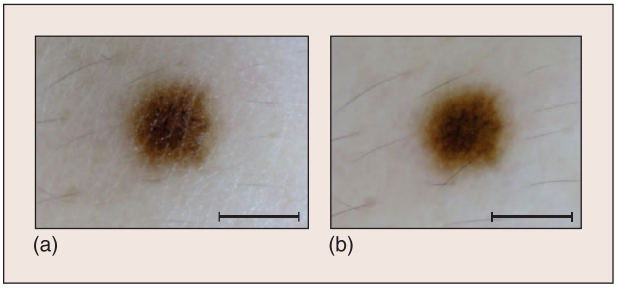

Fig. 6. Dermoscopic images of a mole with diameter of 2mm: (a) without cross-polarization detection and (b) with cross-polarization detection (scale bar: 2 mm).

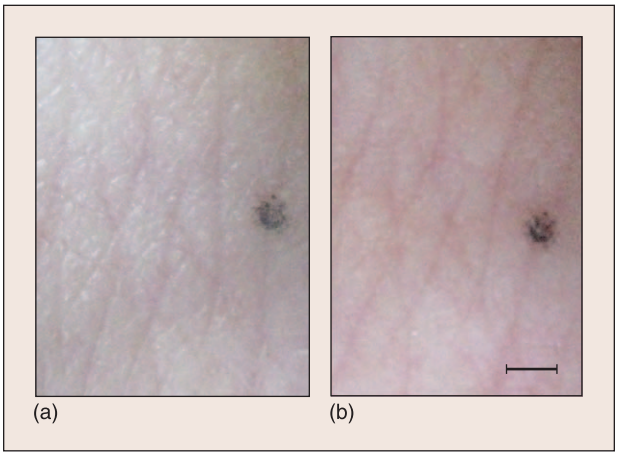

Fig. 7. Dermoscopic images of blood vessels underneath the skin: (a) without cross-polarization detection and (b) with cross-polarization detection (scale bar: 1 mm).

(part 6), one can change the focal length of the lenses in order to focus the image.

The mechanical design meets all the optical requirements:

- Cross-polarization detection is guaranteed and eliminates specular reflection;
- The components fit well together with the LED array and ensure effective light illumination;
- The circuit connects to an on-off switch for easy manipulation;
- Extension and retraction of the circular mount allows the tissue area to be brought into focus; and
- The exposed rim of the view corridor port includes threads for engaging external cameras via a standard Canon lens adapter.

Results

The prototype of the system was designed with SolidWorks and was manufactured by Beijing Jingweili Plastic Model Ltd., China. We used the finished dermoscope to observe human pigmentation lesions on the skin surface and captured the images using a digital camera (Canon Powershot A590). Fig. 6a shows dermoscopic images of a 2 mm diameter mole taken in the absence of polarizers, in which the reflection and folding of the skin surface can be seen clearly. We can observe some of the fine structure, such as the skin surface texture; however, observation of the pigment distribution is seriously compromised due to the strong direct reflection of light from the stratum corneum. Fig. 6b is a cross-polarized microscopic photograph of the same mole. Compared to Fig. 6a, the reflected light coming directly from the skin surface was greatly reduced. We can see that the pigmentation of the mole more clearly, and the edges of the mole before it fades into areas of healthy skin can also be seen. In addition, by using the cross-polarized dermoscope, the superficial skin capillaries could also be observed (see Fig. 7), which can help identify the vascular structure and provide an auxiliary diagnosis of vascular tumors.

In this work, we only utilized white light illumination, color CCD camera recordings, and cross-polarization imaging to access the information from the deeper skin layers. It should be noted that, due to the different absorption/scattering/fluorescent efficiencies of the tissue components, further diagnostic information could be obtained by using spectral illumination/detection [11], [12], [16], [17].

Conclusions

In this paper, the systematic design of a cross-polarized dermoscope is described. We used cross-polarization principles to eliminate the use of an oil medium for superficial reflection cancellation. The system illumination and imaging performance was evaluated using optical simulation to obtain the optimal mechanical parameters. Through the application of polarized illumination and cross-polarization imaging, the dermoscope acquired images from the inner layers of the skin, thereby revealing structures in deeper skin layers, such as pigmentation and capillary blood vessels. The system may help physicians to improve their diagnoses through enhanced dermatological imaging.

Acknowledgments: The authors thank Dr. Thomas FitzGibbon and Shawn Casey for comments and suggestions on earlier drafts of the manuscript.

References

[1] "Cancer facts & figures 2009," The American Cancer Society, [Online] Available: http://www.cancer.org.

[2] M. Tanaka, "Dermoscopy," *The Dermatology*, vol. 33, pp. 513-517, 2006.

[3] Yaroslavsky, V. Neel, and R. R. Anderson., "Fluorescence polarization imaging for delineating nonmelanoma skin cancers," *Optics Letters*, vol. 29, pp. 2010-2012, 2004.

[4] A. A. Marghoob, L. D Swindle, C. Z. M. Moricz, F. A. S. Negron, B. Slue, A. C. Halpern, and A. W. Kopf, "Instruments and new technologies for the in vivo diagnosis of melanoma," *Jour. American Academy of Dermatology*, vol. 49, pp. 777-797, 2003.

[5] C. Benvenuto-Andrade, S. W. Dusza, A. L. C. Agero, A. Scope, M. Rajadhyaksha, A. C. Halpern, and A. A. Marghoob, "Differences between polarized light dermoscopy and immersion contact dermoscopy for the evaluation of skin lesions," *Archives of Dermatology*, vol. 143, pp. 329-338, 2007.

[6] S. L. Jacques, J. R. Roman, and K. Lee, "Imaging superficial tissues with polarized light," *Lasers in Surgery and Medicine*, vol. 26, pp. 119-129, 2000.

[7] R. Anderson, "Polarized light examination and photography of the skin," *Archives of Dermatology*, vol. 127, pp. 1000-1005, 1991.

[8] S. L. Jacques, J. C. Ramella-Roman, and K. Lee, "Imaging skin pathology with polarized light," *Jour. Biomedical Optics*, vol. 7, p. 329, 2002.

[9] M. H. Smith, P. D. Burke, A. Lompado, E. A. Tanner, and L. W. Hillman, "Mueller matrix imaging polarimetry in dermatology," *Proc. SPIE Conference 2000*, pp. 210-216.

[10] J. A. Muccini, N. Kollias, S. B. Phillips, R. R. Anderson, A. J. Sober, M. J. Stiller, and L. A. Drake, "Polarized light photography in the evaluation of photoaging," *Jour. American Academy of Dermatology*, vol. 33, pp. 765-769, 1995.

[11] R. S. Gurjar, V. Backman, L. T. Perelman, I. Georgakoudi, K. Badizadegan, I. Itzkan, R. R. Dasari, and M. S. Feld, "Imaging human epithelial properties with polarized light-scattering spectroscopy," *Nature Medicine*, vol. 7, pp. 1245-1248, 2001.

[12] A. N. Yaroslavsky, V. Neel, and R. Anderson, "Demarcation of nonmelanoma skin cancer margins in thick excisions using multispectral polarized light imaging," *Jou. Investigative Dermatology*, vol. 121, pp. 259-266, 2003.

[13] S. A. Burns, A. E. Elsner, M. B. Mellem-Kairala, and R. B. Simmons., "Improved contrast of subretinal structures using polarization analysis," *Investigative Ophthalmology & Visual Science*, vol. 44, pp. 4064-4068, 2003.

[14] C. Massone, A. Di Stefani, and H. P. Soyer, "Dermoscopy for skin cancer detection," *Current Opinion in Oncology*, vol. 17, pp. 147-153, 2005.

[15] R. P. Braun, H. S. Rabinovitz, M. Oliviero, A. W. Kopf, and Jean-Hilaire Saurat, "Dermoscopy of pigmented skin lesions," *Jour. American Academy of Dermatology*, vol. 52, pp. 109-121, 2005.

[16] B. Jung, B. Choi, A. J. Durkin, and J. S. Nelson. "Method and apparatus for characterization of chromophore content and distribution in skin using cross-polarized diffuse reflectance imaging," ed: US Patent 7400754, 2008.

[17] B. Jung, B. Choi, A. J. Durkin, K. M. Kelly, and J. S. Nelson, "Characterization of port wine stain skin erythema and melanin content using cross-polarized diffuse reflectance imaging," *Lasers in Surgery and Medicine*, vol. 34, pp. 174-181, 2004.

Hening Wang received her B.S. degree in Biomedical Engineering from Shanghai Jiao Tong University in 2010. She is currently a Ph.D. candidate in Dr. Peng Xi's research group at Peking University, where her research is on the application of nanomaterials in optical microscopy.

Xin Xu received her B.S. degree in Biomedical Engineering from Shanghai Jiao Tong University in 2009. She is currently a Ph.D. candidate in the School of Biomedical Engineering, Science and Health Systems at Drexel University, where her research is on the use of piezoelectric cantilevers for cancer detection.

Xiaoqin Li received his B.Sc. degree in Biomedical Engineering from Shanghai Jiao Tong University in 2011. He is currently a Ph.D. candidate in the biomedical engineering system research group at the University of North Carolina at Charlotte, where his research is on 3-D Human motion analysis and biomechanics.

Peng Xi (xipeng@coe.pku.edu.cn) received the Ph.D. degree in Optical Engineering from Shanghai Institute of Optics and Fine Mechanics, Chinese Academy of Sciences in 2003. He is currently an Associate Professor at Peking University. His research interests include biomedical optics, nonlinear optical microscopy, and optical nanoscopy.

Qiushi Ren received his Ph.D. Degree in 1990 at Ohio State University. Dr. Qiushi Ren became a faculty member of the Department of Biomedical Engineering with an adjunct appointment in the Department of Ophthalmology and Bascom Palmer Eye Institute of University Miami before joining the University of California, Irvine. He then returned to China and the Department of Biomedical Engineering at Shanghai Jiao Tong University and is currently the Head of the Department of Biomedical Engineering, College of Engineering, at Peking University.